Causes of drying trends in northern hemispheric land areas in reconstructed soil moisture data

B. Mueller, X. Zhang

Supporting information

S1. Soil moisture simulated by land-surface models vs observational soil moisture

In this study, we use soil moisture simulated by four different land-surface models (LSMs) since long-term, global direct observations of soil moisture are lacking. A global satellite-derived soil moisture product has been developed recently (Dorigo et al. 2010). Here we provide some comparison between soil moisture simulated by the four LSMs with this satellite-derived soil water index from the European Space Agency's (ESA) Climate Change Initiative (CCI). The CCI-dataset has been derived from remotely sensed data of active and passive microwave spaceborne instruments and covers 35 year (http://www.esa-soilmoisture-cci.org/node/145). Some of the short-comings of satellite-derived soil moisture are the shallow penetration depth (about 2cm) of the sensors, a complicated derivation of soil moisture from the actual observed variables, as well as possible problems with temporal inhomogeneities due to the merging of different products. Figure S1 shows the time-series of CCI-data and the average of the LSM-output over the common time period 1979-2008. Both datasets have been standardized and averaged over the three northern hemispheric land-areas. In dry and combined regions, the two datasets correspond quite well in their overall variability, with correlations of 0.61 and 0.42 in dry and combined regions, respectively. Both datasets show significant negative trends in the dry region. Both datasets show similar trend in the combined regions though the trend in CCI-data is not significant at the 5%-level. The variability in the wet region is very small.

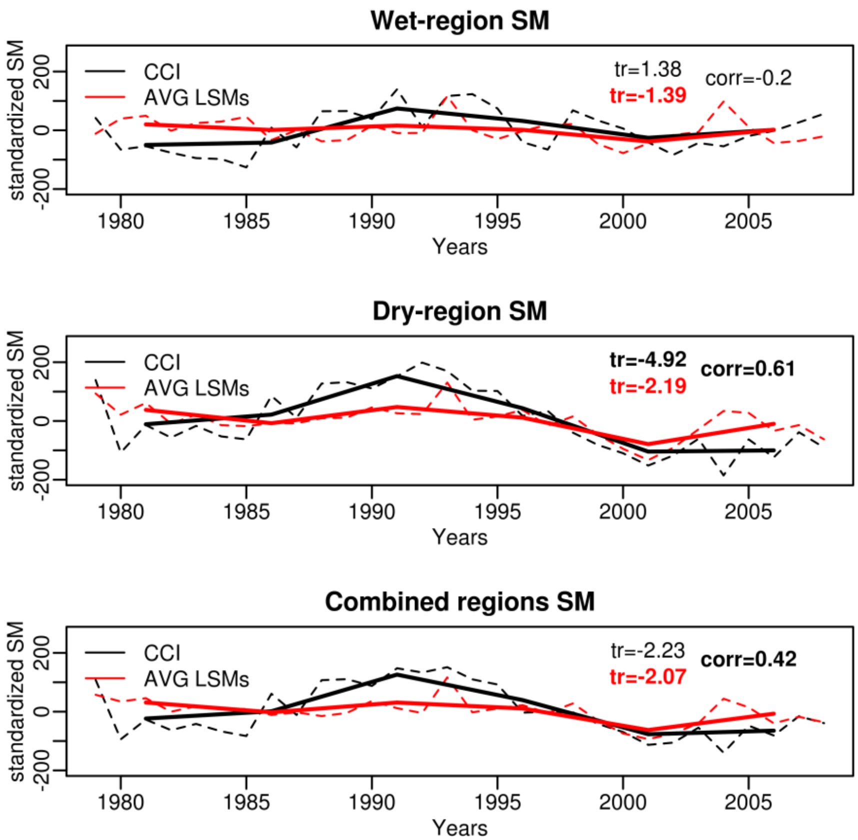

Figure S1: Time series of regional average standardized soil moisture from the LSMs and from satellite retrievals (CCI merged dataset). Solid lines are 5-year averages and dashed lines are annual values. The numbers in the right top are the trends (tr) and the correlation coefficients (corr), with bold values indicating statistical significance at the 5%-level. The Sen's slope estimator and Mann-Kendall test are used for trend calculation.

S2. CMIP5 simulations

We use model simulations from the CMIP5 multi model ensemble for which both historical anthropogenic plus natural (ALL) forcing and historical natural (NAT) forcing were available to estimate forced response patterns. We only select models with at least three runs. The resulting ensemble includes 37 ALL simulations and 37 NAT simulations (see Table S1). The soil depth varies considerably among the models. For the future projection of soil moisture, we used 29 simulations for the Representative Concentration Pathway (RCP) 4.5 scenario (Meinhausen et al. 2011). The number of runs used to estimate future trends are given in brackets behind the number of simulations in Table S1.

Models for signal estimation	**Modelling center**	**Maximum total soil depth**	**Number of simulations**
CCSM4	National Center for Atmospheric Research (NSF/DOE NCAR), Boulder, US	89.0 m	4 (4)
CNRM-CM5	Centre National de Recherches Meteorologiques, Meteo-France, Toulouse, France and Centre Europeen de Recherches et de Formation Avancee en Calcul Scientifque (CERFACS), Toulouse, France	12.2 m	6 (1)
CSIRO-Mk3.6.0	Australian Commonwealth Scientific and Industrial Research Organization Marine and Atmospheric Research (Melbourne, Australia) in collaboration with the Queensland Climate Change Centre of Excellence (QCCCE), Brisbane, Australia	4.6 m	5 (5)
CanESM2	Canadian Centre for Climate Modelling and Analysis, Canada	2.5 m	5 (4)
GISS-E2-H	NASA/ Goddard Institute for Space Studies, New York, US	5.7 m	5 (3)
GISS-E2-R	NASA/ Goddard Institute for Space Studies, New York, US	5.7 m	9 (9)
IPSL-CM5A-LR	Institut Pierre Simon Laplace, Paris, France	7.4 m	3 (3)
Total number of simulations			37 (29)

Table S1: List of CMIP5 models used for signal estimation, corresponding total depth of soil layer and number of simulations used to estimate the ALL and NAT signals (number in last column) and under the RCP4.5 scenario (number in brackets in last column).

We use 380 fifty-five year samples from 40 CMIP5 control simulations to estimate natural internal variability. The considered models and runs are listed in Table S2.

Model name	**Run**	**Modelling center**	**Model name**	**Run**	**Modelling center**
ACCESS1-0	r1i1p1	CSIRO-BOM	GISS-E2-R	r1i1p1	NASA GISS
ACCESS1-3	r1i1p1	CSIRO-BOM	GISS-E2-R	r1i1p141	NASA GISS
BNU-ESM	r1i1p1	GCESS	GISS-E2-R	r1i1p142	NASA GISS
CCSM4	r1i1p1	NCAR	GISS-E2-R	r1i1p2	NASA GISS
CCSM4	r2i1p1	NCAR	GISS-E2-R	r1i1p3	NASA GISS
CESM1-BGC	r1i1p1	NSF-DOE-NCAR	HadGEM2-ES	r1i1p1	MOHC (additional realizations by INPE)
CESM1-CAM5	r1i1p1	NSF-DOE-NCAR	IPSL-CM5A-LR	r1i1p1	IPSL
CESM1-FASTCHEM	r1i1p1	NSF-DOE-NCAR	IPSL-CM5A-MR	r1i1p1	IPSL
CESM1-WACCM	r1i1p1	NSF-DOE-NCAR	IPSL-CM5B-LR	r1i1p1	IPSL
CMCC-CM	r1i1p1	CMCC	MIROC-ESM-CHEM	r1i1p1	MIROC
CMCC-CMS	r1i1p1	CMCC	MIROC-ESM	r1i1p1	MIROC
CNRM-CM5	r1i1p1	CNRM-CERFACS	MIROC5	r1i1p1	MIROC
CSIRO-Mk3-6-0	r1i1p1	CSIRO-QCCCE	MPI-ESM-LR	r1i1p1	MPI-M
CanESM2	r1i1p1	CCCma	MPI-ESM-MR	r1i1p1	MPI-M
GFDL-CM3	r1i1p1	NOAA GFDL	MPI-ESM-P	r1i1p1	MPI-M
GFDL-ESM2G	r1i1p1	NOAA GFDL	MRI-CGCM3	r1i1p1	MRI
GFDL-ESM2M	r1i1p1	NOAA GFDL	NorESM1-M	r1i1p1	NCC
GISS-E2-H	r1i1p1	NASA GISS	NorESM1-ME	r1i1p1	NCC
GISS-E2-H	r1i1p2	NASA GISS	bcc-csm1-1-m	r1i1p1	BCC
GISS-E2-H	r1i1p3	NASA GISS	bcc-csm1-1	r1i1p1	BCC

Table S2: Model names and run members of control simulations used to estimate the internal variability.

Supplementary Figure S2 and S3 and Tables S3 – S5

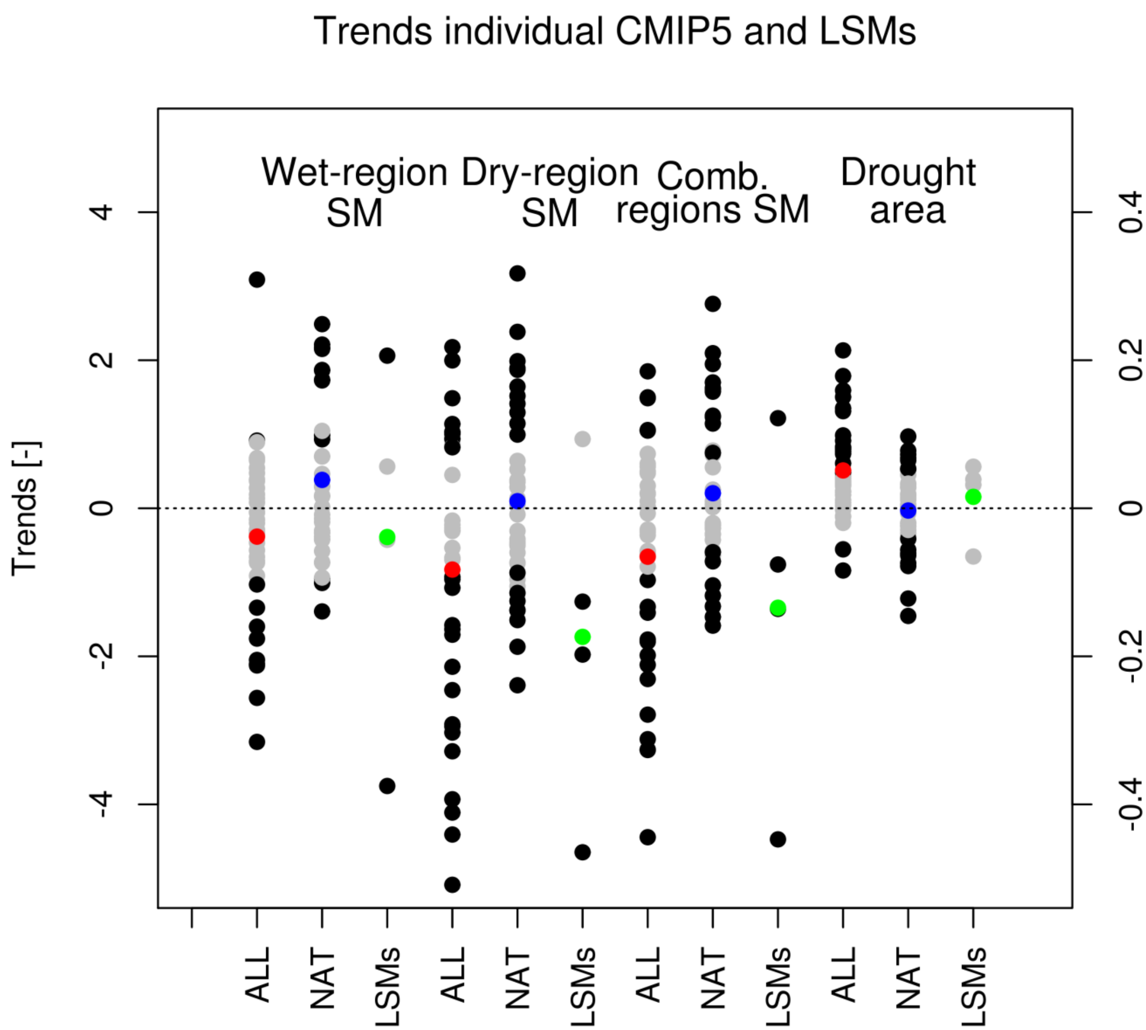

Figure S2: Trends of individual CMIP5-simulations (ALL and NAT) and LSMs. Grey and black dots denote trends in individual simulations, and black indicates that the trend is significant at the 95%-level (Sen's slope estimator and Mann-Kendall test).The colored dots indicate the average of the trends. Note that Figure 3 of the main manuscript shows trends of the ensemble-average time-series which does not correspond to the average of individual trends. The left axis is standardized soil moisture (no units) and the right axis area of drought trends (in percent).

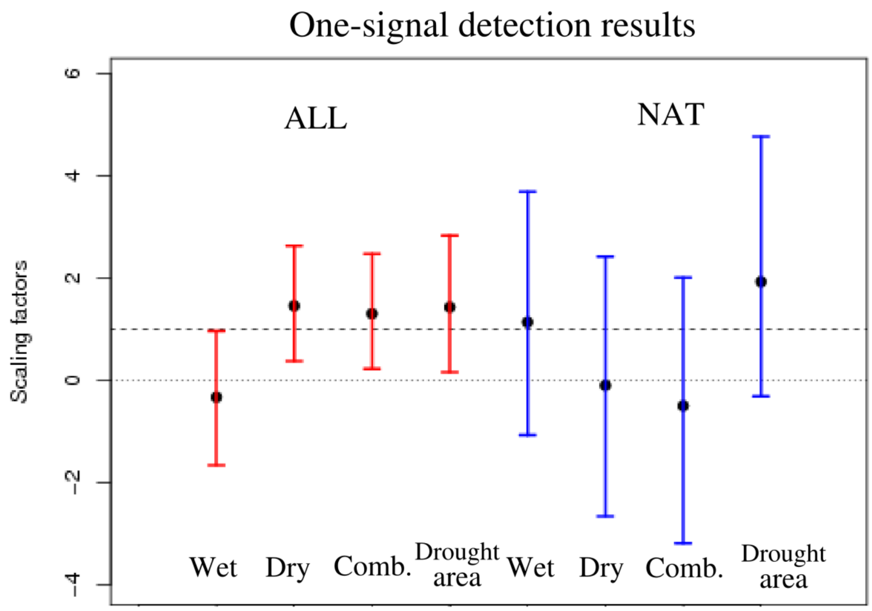

Figure S3: Scaling factors and their 90% confidence intervals obtained from the single-signal analysis for ALL (red) and NAT (blue) forcings based on the average of the LSMs. Results are shown for soil moisture changes in wet, dry and combined area as well as the area affected by drought. The best estimates of the scaling factors are indicated with a dot and the confidence intervals with whiskers. The dashed line highlights one and the dotted line zero. Confidence intervals including one but excluding zero indicate that the change is detected and consistent with the response to the respective forcing.

	CMIP ALL		CMIP NAT	
	positive	negative	positive	negative
Dry-region SM	24.3%	43.2%	29.7%	21.6%
Wet-region SM	5.4%	24.3%	27.0%	8.1%
Combined regions SM	13.5%	35.1%	29.7%	18.9%
Drought area	43.2%	5.4%	18.9%	21.6%

Table S3: Percentage of simulations with trend significant at the 5% level in dry, wet and combined regions soil moisture (SM) and area affected by drought.

Trends in LSMs	Wet-region SM	Dry-region SM	Combined regions SM
Original split used throughout the manuscript	0.54	**-1.76**	**-1.15**
50% wet / 50% dry split	0.43	**-1.74**	**-1.15**

Table S4: Sensitivity of trends in standardized soil moisture anomalies in LSMs to definition of wet and dry areas. Bold values are significant at the 5%-level.

	LSMs	AVERAGE	ORCH	LPJ	OCN	VIC
1-signal	ALL wet	0	1708	0	0	0
	ALL dry	1932	0	0	2000	327
	ALL combined	1801	277	0	2000	0
	ALL drought area	576	0	0	1760	1355
	NAT wet	0	1969	0	33	0
	NAT dry	0	0	62	1457	0
	NAT combined	0	0	0	1173	0
	NAT drought area	46	0	0	167	1177
2-signal	ANT wet	0	1838	0	639	0
	ANT dry	1977	4	0	2000	1425
	ANT combined	1976	78	0	2000	8
	ANT drought area	1166	0	0	1940	2000
	NAT wet	0	1838	0	859	0
	NAT dry	371	0	92	2000	1425
	NAT combined	230	78	0	2000	8
	NAT drought area	888	0	0	1579	2000

(grey)	Less than 10% detected
(light orange)	10-50%
(orange)	50-90%
(red)	90-100%

Table S5: Same as Table 1 in the main manuscript but with results for individual LSMs added. Number of times detection occurred from 2000 different combinations of control run data used for the estimate of internal variability (2000 bootstraps). The results are color-coded for easier understanding.

References

Dorigo WA, Scipal K, Parinussa RM, Liu YY, Wagner W, de Jeu RAM and Naeimi V (2010) Error characterisation of global active and passive microwave soil moisture data sets. Hydrol Earth Syst Sci, 14, 2605-2616, 10.5194/hess-14-2605-2010.

Meinshausen, M, Smith SJ, Calvin KV, Daniel JS, Kainuma MLT, Lamarque JF, Matsumoto K, Montzka SA, Raper SCB, Riahi K, Thomson AM, Velders GJM and van Vuuren D (2011) The RCP Greenhouse Gas Concentrations and their Extension from 1765 to 2300. Climatic Change (Special Issue), DOI: 10.1007/s10584-011-0156-z.